Dynamic Article Links ►

Cite this: DOI: 10.1039/c0xx00000x

www.rsc.org/XXXXX

PAPER

Two and three input molecular logic operations mediated by a novel azo-azomethine based chromogenic probe through intramolecular charge transfer processes

Khatereh Rezaeian and Hamid Khanmohammadi*

Received (in XXX, XXX) Xth XXXXXXXXX 20XX, Accepted Xth XXXXXXXXX 20XX
DOI: 10.1039/b000000x

A novel azo-azomethine based chromogenic receptor containing diaminomaleonitrile fragment and pyridine ring has been designed and synthesized for fabrication of multifunctional molecular logic circuits. The current system exhibited absorption response profiles varying significantly with different anionic and cationic inputs in DMSO-water (9:1) through the modulation of intramolecular charge transfer (ICT) processes. The responsive mechanism of the system was also explored and elucidated. Importantly, the changes of absorbance output signals at particular wavelengths in response to F^- and Zn^{2+} as two chemical inputs provided opportunities for elaboration of 2-bit Boolean binary logic functions like OR and INHIBIT gates. Successfully, a 3-input logic network composed of EnNOR combinational circuit could also be interpreted using F^-, Zn^{2+} and Cu^{2+} as input variables. Furthermore, the integration of fundamental logic functions was discussed to establish complex logic circuits including reconfigurable 2-bit logic gates and the three-input combinatorial logic circuits. More interestingly, based on the reversible and reproducible switching behaviour of the fluoride interaction with Ca^{2+}, we presented a potential "Write–Read–Erase–Read" memory function possessing multi-write ability.

Introduction

Research in the area of signal communication at molecular level has recently gained much significance in sustaining the development of innovative materials for data storage and processing. In 1988, Aviram suggested the use of molecules in molecular electronic devices for memory, logic and amplification.[1] In 1993, de Silva and co-workers presented the first unambiguous report on the possibility of the individual molecule performing complicated Boolean logic operations with specified set of ionic or molecular inputs.[2] Thereafter, tremendous efforts have been directed toward the fabrication of molecular systems capable of performing binary arithmetic and logical operations.[3] Hence, the realization of molecular devices with capability of mimicking logic gates opened up new opportunities to overcome the limitation of the conventional silicon-based electronics in miniaturization down to the nano scale size.[4]

Recently, an ample number of molecular logic devices such as logic gates (AND, OR, XOR, NAND, NOR, INHIBIT, half-adder and half-subtractor), molecular keypad locks and information storage devices have been widely explored.[5] However, there is a paucity of reports regarding the construction of sequential logic circuits with memory function.[5f] Hence, realization of some advanced logic in the form of memory functions like "Write–Read–Erase–Read" remains a significant challenge in the field of molecular information technology. [5g-i]

Logic gates are switches whose output state (*0* or *1*) depends on the input conditions (*0* or *1*).[3a] Typically, in most molecular logic gates, the output signals can be encoded as absorption or photoluminescence and their inputs are rather drivers, including light, temperature, ions and certain molecules.[3c,4e,6] Regarding ionic inputs, myriad of paradigms have been well documented. However, most of them are known for two or multi-cation[7] driven species and there is a paucity of reports based on anionic inputs in the contemporary literature.[8] Furthermore, extensive investigations have been devoted toward logic gate applications based on dual receptor molecules with different dedicated binding sites for cations and anions.[3c,9] In particular, although literatures are replete with excellent examples of molecular analogous of many logic gate functions, only few of them are on the basis of colorimetric receptors.[4a,10] Accordingly, the colorimetric receptors based molecular logic gates are of elevated interest among chemists.

Department of Chemistry, Faculty of Science, Arak University, Arak 38156 8 8349, Iran.
E-mail: h-khanmohammadi@araku.ac.ir; Fax: (+)98-863- 4173406; Tel: (+)98-863-2777401

† Electronic Supplementary Information (ESI) available: Characterization data of all compounds, UV-Vis spectrophotometric titrations, stoichiometric determination by Benesi–Hildebrand method, Job's plot, ^1H NMR titration, IR spectra of **1** with cations and reversibility of receptor with various ions. See DOI: 10.1039/b000000x/

More recently, the combination of individual logic systems inside a single molecule has induced great interests for construction of molecular logic circuits capable of executing some special arithmetic operations.[11] Such integration has been anticipated to be an elegant way to further widen logic gate applications. Latest advances in combinational systems involving two or more outputs inspired us to design and construct the molecular system that mimic the logic functions in presence of cations and anions. Such integrated logic gates in a single molecular switch with unprecedented performance have potential implications in the progress of electronic and photonic devices.[5c]

Until now, many receptors capable of performing most of the common logical operations have been actively studied.[7-10] However, reports for molecular logic gate based on azo scaffold are still scarce. In 2010, chung *et al.* reported a novel bifunctional chromogenic calix[4]arene containing bistriazoles and azophenols moieties to construct a combinational logic circuit at the molecular level.[12] Furthermore, Wang and Ha applied new ortho-substituted azobenzene derivatives for fluorescent molecular logic gates operated by two chemical inputs OH$^-$ and metal cations.[13] In pursuit of these, we have designed and synthesized a new azo-azomethine based colorimetric receptor, **1**, (Scheme 1) and investigated the logic responses by using appropriate combinations of anions and cations as inputs in DMSO-water (9:1). To the best of our knowledge, this is the first report where azo-azomethine receptor has been considered as molecular logic gate. However, a number of reports have been published on azo-azomethine compounds for other applications.[14] Remarkably, on the basis of the response profiles of **1** in terms of absorption, we have fabricated a unique molecular system capable of executing multiple and complex logic functions such as OR, EnNOR, INH, IMP via varying the combination of ionic inputs. Interestingly, the colorimetric and spectral responses can be switched back and forth by successively addition of F$^-$ and Ca^{2+} which may be illustrated by a complementary “IMPLICATION/INHIBIT” molecular logic gate using F$^-$ and Ca^{2+} as chemical inputs. Further, this reversible and reproducible switching behaviour prompted us to consider the synthesized azo-azomethine receptor as a molecular system exhibiting “Write–Read–Erase–Read” and “Multi-Write” functions.

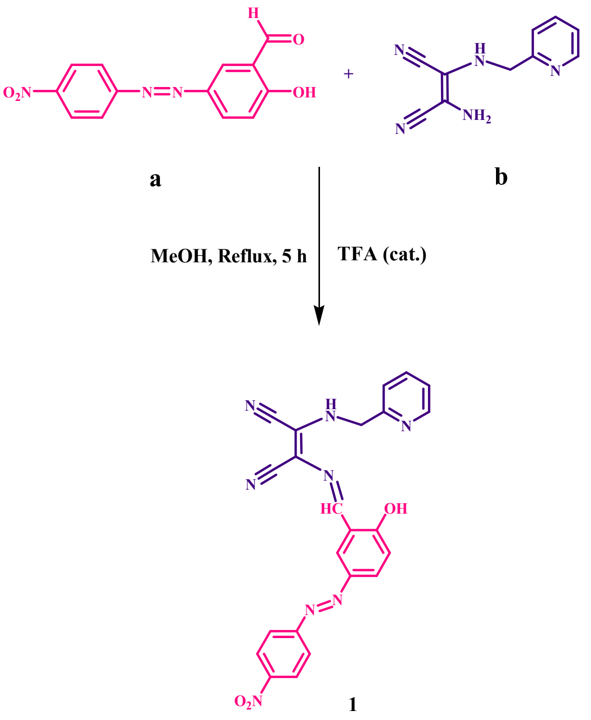

Scheme 1 Synthesis of receptor **1**.

Results and discussion

Molecular design and synthesis

The strategy employed in the design of receptor is as follows. Firstly, in devised compound, diaminomaleonitrile fragment is conjugated not only with azo-azomethine scaffold but also with pyridine ring. This would endow the system with the ability to provide the efficient metal binding sites via disposal of nitrogen and oxygen heteroatoms. Secondly, the introduction of highly electron-withdrawing nitrile and NO_2 groups into the backbone of sensing molecule appreciably augments the acidity of active NH and OH sites; thereby promoting the anion affinity in aqueous organic environment. Thirdly, the synthesized receptor is equipped with nitro-azobenzene moiety as chromogenic signaling subunit to achieve “naked-eye” detection. Therefore, we envisage that the devised molecule can as well be served as proficient receptor for interacting with both anions and cations. Notably, these circumstances provide opportunities for **1** to proceed upon logic operations with multiple outputs by utilizing two and three combinational inputs through modulating intramolecular charge transfer (ICT) processes.

The synthesis of novel azo-azomethine receptor was achieved via condensation reaction of 2-Amino-3-[(2-pyridylmethyl)amino]-2(Z)-butene-1,4-dinitrile (b) with 1-(3-formyl-4-hydroxyphenylazo)-4-nitrobenzene (a) in excellent yield as depicted in Scheme 1. The target compound was characterized using standard spectroscopic techniques (ESI†).

Spectroscopic studies involving anions

Initially, the chemosensing properties of receptor **1** were assessed visually and then by UV-Vis spectrophotometry in DMSO-water (9:1) upon the addition of various anions such as F$^-$, Cl$^-$, Br$^-$, I$^-$, ClO_4^-, AcO$^-$, NO_3^-, HSO_4^-, N_3^-, NO_2^- and $H_2PO_4^-$ as their TBA salts. As illustrated in Fig. 1, the UV-Vis absorption spectrum of **1** (2×10^{-5} mol L^{-1}) gives rise to an intense band centred at 394 nm, attributed to the π→π* transition of chromophores and less intense absorption band at 585 nm corresponding to the n→π* transition and also intramolecular charge transfer (ICT) interaction involving the whole molecule of the receptor.[14b] On incremental increase of F$^-$, the absorption band at 394 nm remarkably decreased. This change was accompanied with significant enhancement of the absorbance at 585 nm and emergence of new band at 480 nm. A distinct isosbestic point was observed at 445 nm, indicating strong interaction between fluoride and receptor. These observations were in accordance with discernable colour change from light green to dark blue. It is worthy to note that AcO$^-$ and $H_2PO_4^-$ induced similar colour

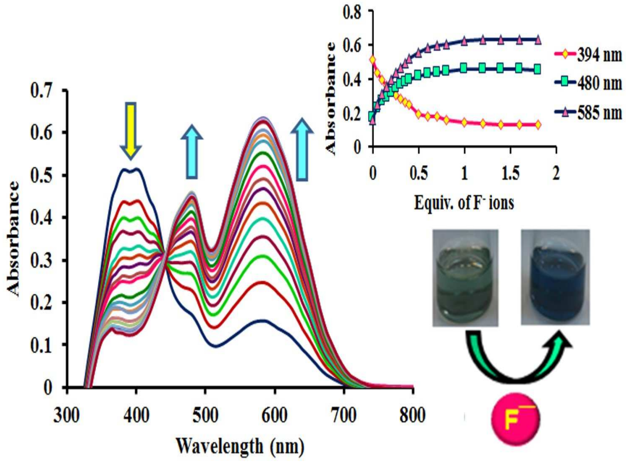

Fig. 1 UV-Vis titration of **1** (2×10^{-5} mol L^{-1}) in DMSO-water (9:1) with incremental addition of standard solution of TBAF. Inset showing the binding isotherm at selected wavelengths in DMSO-water (9:1).

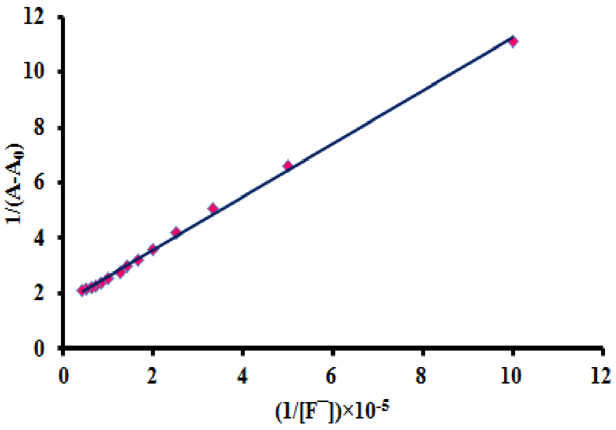

Fig. 2 Benesi–Hildebrand plot of **1** binding with F^- anion associated with absorbance change at 585 nm in DMSO-water (9:1).

change and spectral pattern (Fig. S5, ESI†). Conversely, the addition of other examined anions failed to cause any conspicuous colour and spectral changes. Furthermore, the definite stoichiometric ratio between **1** and aforementioned anions was determined to be 1:1 with the help of Benesi–Hildebrand method[15] and also Job's plot experiments (Fig. S6 and S7, ESI†). Apparently, plotting of $1/[A\text{-}A_0]$ *vs.* $1/[F^-]$ for titration of **1** with TBAF showed linear relationship (Fig. 2), corroborating that **1** interacts with F^- in a 1:1 stoichiometric ratio. Moreover, the deprotonation constants (K) for **1** with F^-, AcO^- and $H_2PO_4^-$ were evaluated from Benesi–Hildebrand equation. Accordingly, the resulting values are summarized in Table 1. It is worth to emphasize that the current system is capable of detecting F^-, AcO^- and $H_2PO_4^-$ in aqueous organic media. It has to be pointed out that the incorporation of highly electron-withdrawing NO_2 substituent along with nitrile groups into the framework of sensing molecule greatly decreases electron density on active sites and renders the hydrogen-bind donors appreciably acidic; thereby promoting the anion affinity.[16] This is the reason why the designed receptor is capable to compete with water molecules to detect the trace amount of mentioned anions in aqueous organic environment.

Table 1 Deprotonation constants (K) for **1** with F^-, AcO^- and $H_2PO_4^-$ in DMSO-water (9:1) as determined by UV-Vis titration techniques.

Anions	K, M
F^-	2.10×10^5
AcO^-	2.14×10^5
$H_2PO_4^-$	2.27×10^5

Encouraged by the above anion sensitive absorbance behaviour, we chose F^- as representative of anions for studying logic operations in subsequent experiments. In the next step, to shed light on the nature of interaction between **1** and fluoride, ^{1}H NMR spectroscopy was conducted. Interestingly, after addition of 1 equiv. of F^-, the signals at 11.58 and 8.84 ppm, attributed to the OH and NH protons, respectively, got thoroughly vanished and simultaneously, the aromatic proton signals underwent upfield shift (Fig. S8, ESI†). The profound upfield shift is ascribed to the considerable augmentation of electron density onto the π-conjugated framework brought by neat proton transfer from receptor to anion.[17] Consequently, the electron density over the deprotonated probe was increased, leading to the enhanced ICT transition from electron rich O^- and N^- to the electron deficient nitro and nitrile moieties. This hypothesis was further strengthened by titration of **1** with standard solution of tetrabutylammonium hydroxide, TBAOH, (Fig. S9, ESI†). Evidently, the titration profiles showed close resemblance to that observed with fluoride, reflecting deprotonation phenomenon.[18]

Spectroscopic studies involving cations

The ability of chemosensor **1** to form complexes with Co^{2+}, Ni^{2+}, Cu^{2+} and Zn^{2+} ions was investigated using UV-Vis spectroscopy. Fig. 3 and Fig. 4 depict the representative chromogenic behaviour of **1** (2×10^{-5} mol L^{-1}) toward Cu^{2+} and Zn^{2+} ions as their chloride salts in DMSO-water (9:1). Upon the addition of either Cu^{2+} or Zn^{2+} ions, the broad absorption band at 585 nm was disappeared completely. Thereafter, further sequential addition of target metal

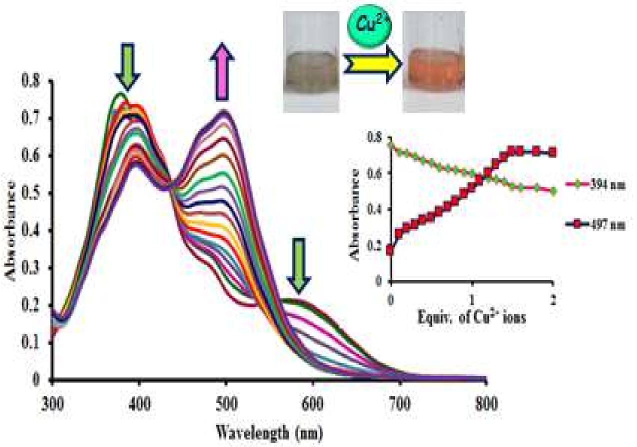

Fig. 3 UV-Vis titration of **1** (2×10^{-5} mol L^{-1}) in DMSO-water (9:1) with incremental addition of Cu^{2+} (0-5 equiv.). Inset showing the binding isotherm at selected wavelengths in DMSO-water (9:1).

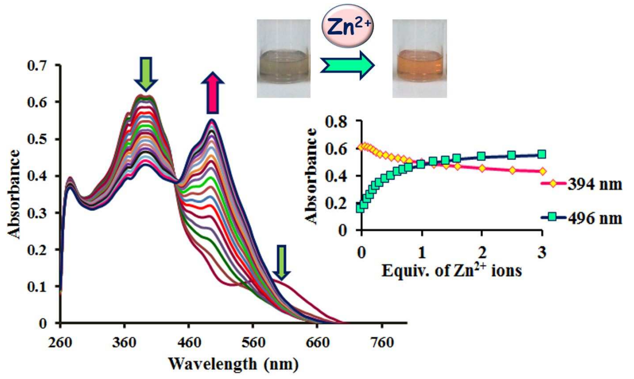

Fig. 4 UV-Vis titration of **1** (2×10^{-5} mol L^{-1}) in DMSO-water (9:1) with incremental addition of Zn^{2+} (0-5 equiv.). Inset showing the binding isotherm at selected wavelengths in DMSO-water (9:1).

cations to the receptor solution induced a gradual decrease of the absorption band at 394 nm and a concomitant growth of new red shifted band centred at *ca.* 495 nm. Notably, the large bathochromically shifted band, originating from the extended ICT process, was responsible for a perceptible colour change from light green to orange as can be seen in photographs.[19] Additionally, distinct isosbestic points at 442 and 445 nm for Cu^{2+} and Zn^{2+}, respectively, are apparent, which indicates the formation of only one active copper or zinc complex with the receptor. Moreover, the titrations of **1** with Co^{2+} and Ni^{2+} afforded similar spectral changes (Fig. S10, ESI†).

It is significant to note that the presence of other examined metal cations including Li^{+}, Na^{+}, K^{+}, Cd^{2+}, Mg^{2+}, Al^{3+}, Hg^{2+}, Pb^{2+}, Cr^{3+}, Mn^{2+}, Ba^{2+}, Fe^{3+} and Ca^{2+} failed to cause any conspicuous spectral changes.

Table 2 Binding constants (K) of Zn^{2+}, Cu^{2+}, Ni^{2+} and Co^{2+} with receptor **1** in DMSO-water (9:1).

Cations	K, M
Zn^{2+}	1.21×10^{5}
Cu^{2+}	3.01×10^{4}
Ni^{2+}	7.22×10^{4}
Co^{2+}	7.68×10^{4}

To further elicit the spectroscopic ratio between **1** and cations, Benesi–Hildebrand method was executed. Plotting of $1/[A-A_0]$ *vs.* $1/[M^{2+}]$ provided straight line, supporting the 1:1 stoichiometry ratio (Fig. S11, ESI†). The 1:1 binding stoichiometry was also substantiated by Job's plot experiment (Fig. S12, ESI†). Assuming 1:1 ratio, the binding constants were also calculated using the Benesi–Hildebrand equation. Accordingly, the resulting values are summarized in Table 2.

To investigate the logic operations of receptor **1**, Cu^{2+} and Zn^{2+} ions were taken as two of the signal inputs. In an effort to gain more detailed information on the nature of binding mode of **1** with cations, Infrared (IR) spectroscopy was employed. The IR spectrum of **1** (Fig. S3, ESI†) shows characteristic band at 3271 cm^{-1}, attributable to the stretching mode of the NH group.[20] The disappearance of this band in the spectrum of **1**-Zn^{2+} (Fig. S13, ESI†) reveals that the NH fragment has been deprotonated and coordinated to the metal ion. The FT-IR spectrum of **1**-Zn^{2+} compared with that of free receptor indicates that the υ(C=N) band at 1618 cm^{-1} is red shifted to lower frequency by 16 cm^{-1}. Also, medium and sharp band at 1556 cm^{-1}, assigned to the υ(C=N) (pyridine ring) vibration, merges into the broad band of

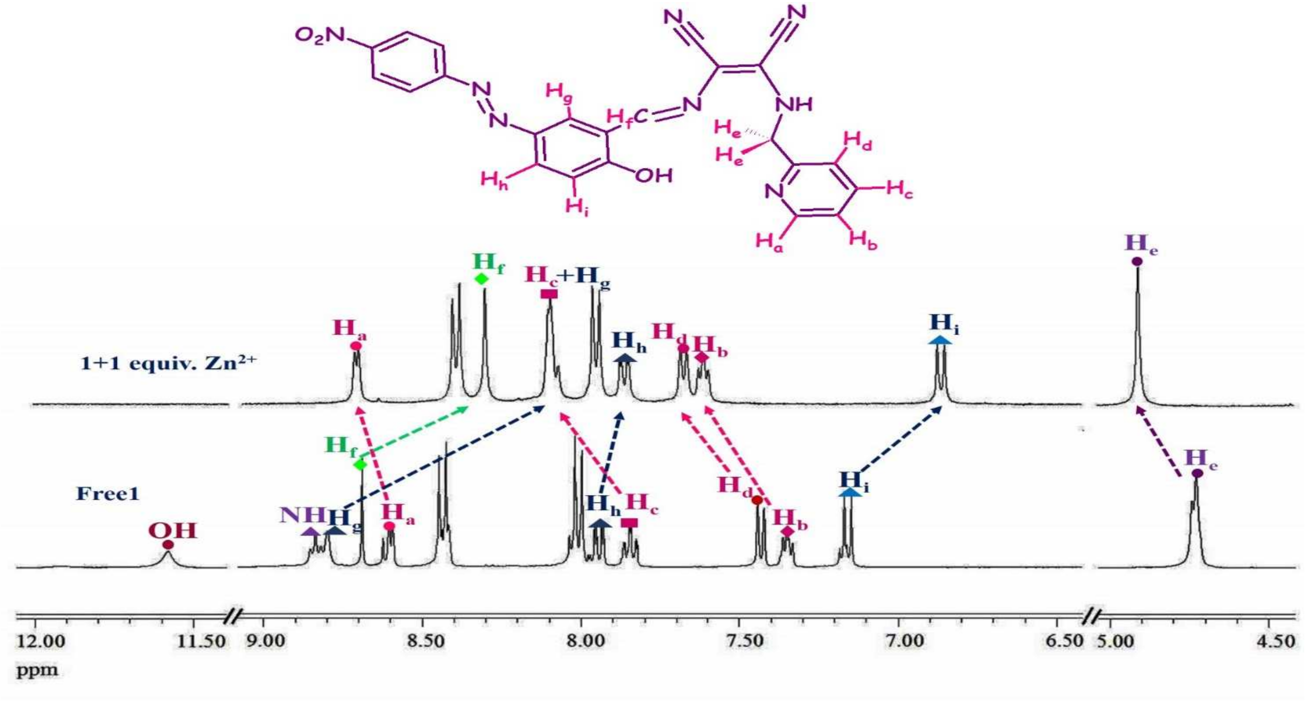

Fig. 5 ^{1}H NMR spectra of **1** in DMSO-d_6 (2×10^{-2} mol L^{-1}) in the absence and presence of 1 equiv. of Zn^{2+}.

azomethine linkage at 1602 cm^{-1}. The observed shifts are consistent with the involvement of nitrogens of azomethine and pyridine in complex formation.[21a] The bonding of the pyridine nitrogen atom is also shown by the presence of the bands at 1010-1030 cm^{-1} and 630-660 cm^{-1} attributable to the ring breathing frequency and the low energy pyridine ring vibrations, respectively.[21b] In addition, upon complexation, significant changes were obtained in the positioning of the υ(C-O) (phenolic) band, reflecting coordination via the oxygen atom. It is noteworthy to mention that similar shift pattern was observed for interaction of **1** with Cu^{2+} ion (Fig. S14, ESI†). Subsequently, in order to strengthen our conclusion based on the findings through IR spectroscopy, ^1H NMR experiment was also applied. Spectra of azo-azomethine receptor before and after treatment with 1 equivalent of Zn^{2+} are shown in Fig. 5. On complexation of **1** with zinc ions, the triplet signal of NH proton at 8.84 ppm and the phenolic proton signal at 11.58 ppm disappeared completely and the singlet associated with CH=N proton was shifted upfield by $\Delta\delta$=-0.39 ppm. Similarly, peaks assigned to the protons of azophenol moiety experienced clear upfield shifts. These observations suggested that the NH and OH groups as well as imine nitrogen (CH=N) of receptor **1** participated to complex with Zn^{2+}.[22a,b] At the same time, addition of Zn^{2+} to the receptor **1** induced considerable downfield shifts in the protons of pyridine and methylene group, supporting the binding of the Pyridyl moiety to the metal ions.[22c] Therefore, in combination with the results of the Job's plot and IR spectroscopy, we propose the formation of 1:1 complex between binding sites of **1** and M^{2+} as illustrated in Scheme 2.

Reversibility of 1 binding to various ions

Reversibility, the ability to regenerate the free probe from the complex, is a very important parameter. Hence, we tested the reversibility of receptor **1** after immersion in F^- and Cu^{2+}/Zn^{2+}, respectively (Fig. S15 and S16, ESI†). To validate the reversible interaction of **1** with F^-, we performed Ca^{2+}-addition experiment.[11a] Similarly, the reversibility of the complexation process for **1** with Cu^{2+}/Zn^{2+} ions was also studied with the chelating agent EDTA.[23] As anticipated, the original colour and absorption spectra of probe **1** binding to F^- and Cu^{2+}/Zn^{2+} could all be recovered immediately. These procedures could be repeated over several cycles which obviously demonstrate the high degree of reversibility. Overall, the results disclosed that the receptor **1** could be reused with proper treatment.

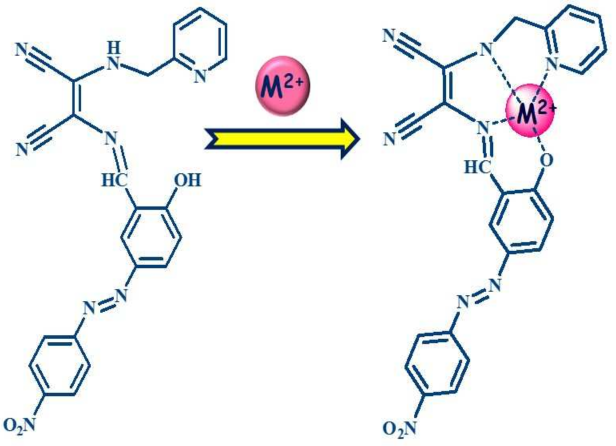

Scheme 2 Proposed binding structure of **1** with M^{2+}.

Construction of logic gate

As discussed above, the UV-Vis absorption spectrum of **1** could be distinctly affected by introduction of different anionic and cationic inputs. This anion/cation sensitive absorbance behaviour provides an opportunity for fabricating the Boolean logic gates and arithmetic calculations at molecular level.

Monitoring the absorption output signals at appropriate wavelengths, a combinatorial logic circuit having OR and INHIBIT logic functions is constructed at monomolecular level using F^- and Zn^{2+} as two chemical inputs. If we choose the absorbance at 488 nm as the output signal (Out1), the OR logic operation can be obtained. As illustrated in Fig. 6, in the absence of any inputs, the absorbance intensity at 488 nm was lower than a predefined threshold level (< 0.3) and accounted for the Boolean value of "*0*", whereas in the presence of either one or both inputs, the absorption intensities of **1** were obviously higher than threshold (> 0.3) corresponding to the Boolean value of "*1*". Also to demonstrate that **1** behaves as INH gate, the output signal at 585 nm has been monitored. The high colorimetric output (Out2) was produced in the presence of F^- (output value was "*1*") and remained low in all other circumstances (output value was "*0*"), Fig. 6. Hence, the absorbance at 585 nm can be utilized for

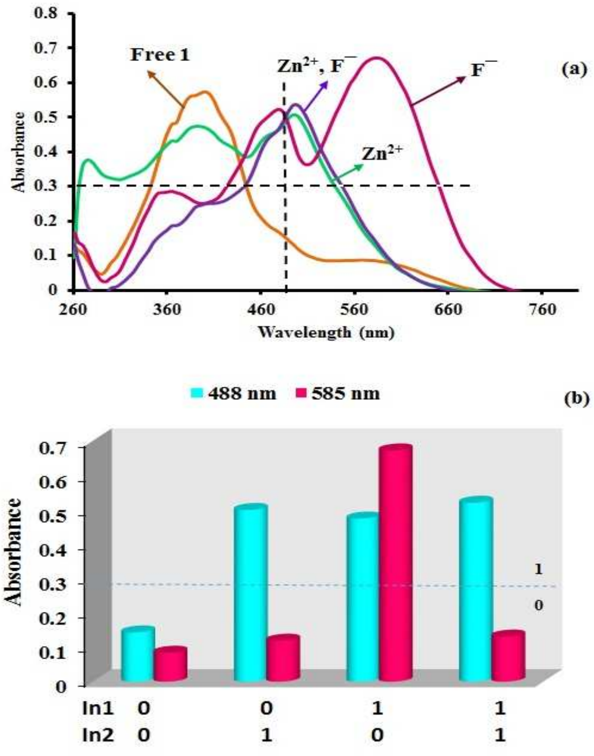

Fig. 6 (a) Absorption spectra of **1** (2×10^{-5} mol L^{-1}) under different input conditions with F^- (In1, 5 equiv.) and Zn^{2+} (In2, 5 equiv.).(b) The changes of absorbance at 488 and 585 nm in the presence of chemical inputs.

the elaboration of INHIBIT logic operation. Consequently, these observations of OR (488 nm) and INH (585 nm) functions have been compiled in the truth table. According to the histogram in Fig. 6, corresponding truth table and the combinatorial logic circuit are presented in Fig. 7.

On the basis of above-mentioned results, receptor **1** can beautifully mimic the function of an INH gate via ICT process. The absorption output (Out2) of **1** was observed in the presence of F^- (In1) at 585 nm and inhibited by the addition of Zn^{2+} (In2). More interestingly, by the introduction of Cu^{2+} as the third input (In3), a three-input combinatorial circuit could be executed in which both Zn^{2+} and Cu^{2+} inputs (In2 and In3) inhibited the absorbance output (Out2) at 585 nm and F^- enabled the device. In the other words, the INH function in Fig. 7 can be extended to the corresponding equivalent logic circuit, enabled NOR (EnNOR) gate. In this regard, Zn^{2+} and Cu^{2+} as two chemical inputs (In2 and In3) are combined through NOR operator. The output of the AND gate is fed by this NOR operator and F^- (In1). Herein, the presence of F^- has the function of control signal which means that whenever it is "*1*", the NOR gate works whereas the gate closes if it is "*0*". This behaviour is typical for enabled NOR (EnNOR) gate.[24]

On the other hand, when Cu^{2+} (In3) acts on the combination of F^- and Zn^{2+}, the absorption output at 488 nm (Out1) still correlates very well with OR logic gate (Fig. 8). Encouraged by these observations, we further endeavoured to construct a more complicated combinational logic circuit by combining three chemical inputs (F^-, Zn^{2+} and Cu^{2+}) and monitoring two different output signals at 488 and 585 nm. Very remarkably, this chemical system converts input strings of three binary digits into output strings of two binary digits. According to the histogram in Fig. 8b, the truth table and combinational logic circuit are shown in Fig. 9. As can be seen, one portion of this logic circuit converts the three inputs into Out1 through OR operations whereas the other fragment transduces the same inputs into Out2 through NOR and AND operations.

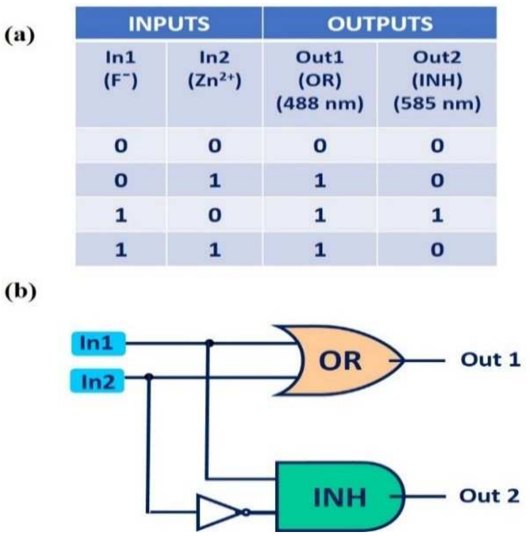
(a)

INPUTS		OUTPUTS	
In1 (F^-)	In2 (Zn^{2+})	Out1 (OR) (488 nm)	Out2 (INH) (585 nm)
0	0	0	0
0	1	1	0
1	0	1	1
1	1	1	0

(b)

Fig. 7 (a) The truth table and (b) the logic circuit for the OR/INH logic gates.

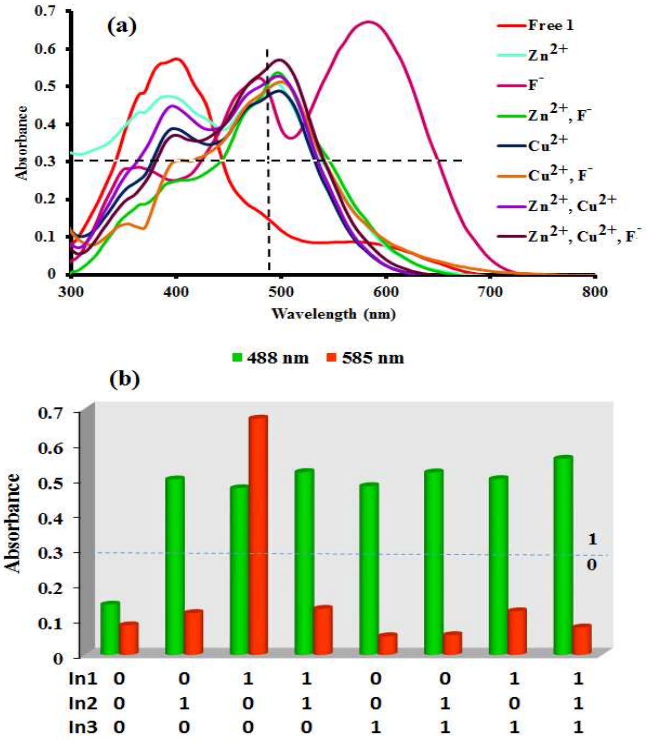

Fig. 8 (a) Absorption spectra of **1** (2×10^{-5} mol L^{-1}) under different input conditions with F^- (In1, 5 equiv.), Zn^{2+} (In2, 5 equiv.) and Cu^{2+} (In3, 5 equiv.). (b) The changes of absorbance at 488 and 585 nm from the eight possible input combinations.

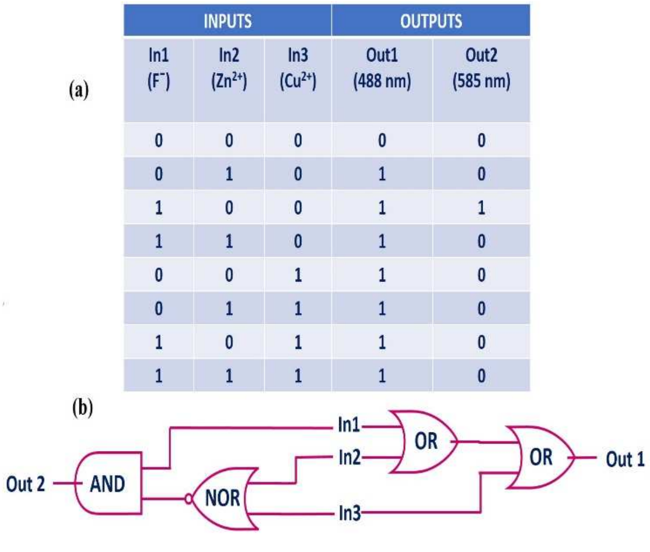
(a)

INPUTS			OUTPUTS	
In1 (F^-)	In2 (Zn^{2+})	In3 (Cu^{2+})	Out1 (488 nm)	Out2 (585 nm)
0	0	0	0	0
0	1	0	1	0
1	0	0	1	1
1	1	0	1	0
0	0	1	1	0
0	1	1	1	0
1	0	1	1	0
1	1	1	1	0

(b)

Fig. 9 (a) The truth table and (b) the three input combinatorial logic scheme.

Most importantly, each state of the logic machine exhibits an interesting reset mechanism. As it was mentioned, addition of F^- resulted in emergence of the absorption bands at 480 and 585 nm, thus acting as ON switch. Subsequently, the F^--induced chromogenic process was fully reversed by the addition of Ca^{2+} cations. In this regard, introduction of Ca^{2+} resulted in vanishing of aforementioned bands at 480 and 585 nm and reappearance of the absorption band at 394 nm, thus acting as OFF state. This type of reversible and reproducible colorimetric switching behaviour correlates very well with INH logic gate by employing F^- and Ca^{2+} as the chemical inputs (InF and InC respectively) and monitoring absorbance at either 480 or 585 nm. While setting the absorbance at 394 nm as another output, an "IMPLICATION" logic gate can also be constructed. Hence, the absorption band at 394 nm has been generated under all circumstances, except in the presence of F^- anion. The IMP logic function output is complementary to an INH gate and is equivalent to the IF-THEN operation and the NOT operation.[25] In this way, the complementary IMP/INH logic functions are realized using **1** and logic circuit is illustrated in Fig. 10. Notably, this reversible colorimetric switch could be repeated consecutively by alternating addition of F^- and Ca^{2+} ions to the receptor solution as depicted in Fig. 11.

Nowadays, the fabrication of this kind of reversible switch is of tremendous interest owing to the significant role in the field of information technology.[5f,26] Thus, according to above observations, we could utilize the current system to design a sequential logic circuit displaying "Write–Read–Erase–Read" behaviour with the help of binary logic (Fig. 12). In the present system, ON state (Out2 =*1*) is defined as the strong absorption at either 480 or 585 nm, whereas the OFF state (Out2 =*0*) corresponds to the weak absorption at identical wavelengths. The two chemical inputs of F^- and Ca^{2+} ions are designated as InF and InC for the Set (S) and Reset (R), respectively. When the Set input is high (S=1), the system writes and memorizes the binary state "*1*". Then, the stored information is erased by Reset input (R=1), resulting in the writing and memorization of binary state "*0*". These reversible and reconfigurable sequences of Set/Reset logic operations can be represented in the form of feedback loop, corroborating the memory feature with "Write–Read–Erase–Read" function through the output signal at either 480 or 585 nm (Fig. 12a and b). Successfully, the remarkable feature of the proposed system is the bi-stability behaviour, "ON-OFF" state, of the azo-azomethine compound and also "Multi-Write" ability without any appreciable degradation in its optical output.

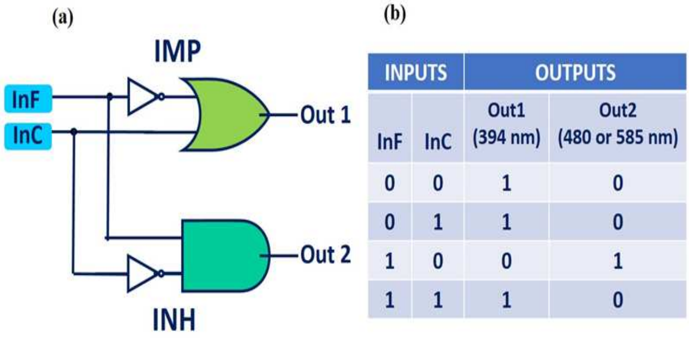

INPUTS		OUTPUTS	
InF	InC	Out1 (394 nm)	Out2 (480 or 585 nm)
0	0	1	0
0	1	1	0
1	0	0	1
1	1	1	0

Fig. 10 (a) The logic circuit and (b) the truth table for the complementary IMP/INH logic gate.

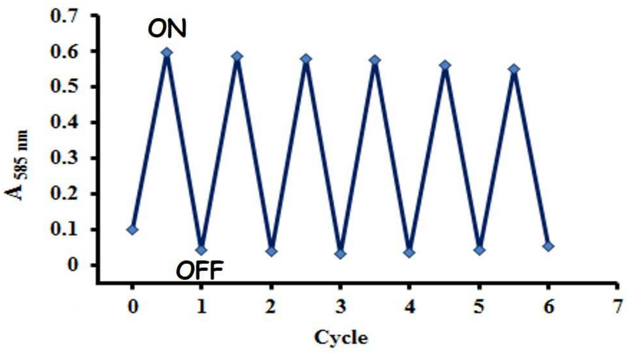

Fig. 11 Reversibility of the receptor **1** (2×10^{-5} mol L^{-1}) with sequential addition of F^- and Ca^{2+}.

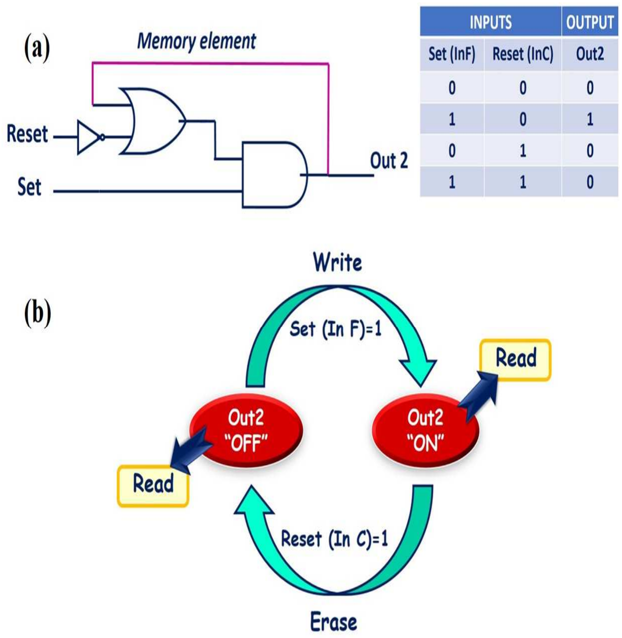

INPUTS		OUTPUT
Set (InF)	Reset (InC)	Out2
0	0	0
1	0	1
0	1	0
1	1	0

Fig. 12 (a) The sequential logic circuit with the memory unit and its truth table.(b) The feedback loop exhibiting reversible logic operations with "Write-Read-Erase-Read" function.

Conclusion

In closing, we have successfully designed and synthesized a new azo-azomethine based chromogenic receptor capable of recognizing both anions and cations in aqueous organic environment. The absorption spectra responses of the probe, which are remarkably sensitive towards anions and metal cations have been investigated in DMSO-water (9:1) solution. In our assay, we also demonstrated that the newly designed molecule can perform basic Boolean operations with anions and cations as chemical inputs and the absorption intensity as the logic output through modulating ICT processes. Notably, multiple and complex logic operations such as OR, EnNOR, INH, IMP have been constructed on the unimolecular platform. Further, combinational logic circuits have also been achieved in absorption mode. Besides, a potential "Write–Read–Erase–Read" memory function possessing multi-write ability has been proposed based on the reversible and reproducible switching behaviour of the fluoride interaction with Ca^{2+} cations. More importantly, it is envisioned that the results described in this report will add a new direction towards the fabrication of more integrated molecular devices with multiple functions.

Experimental

General

All chemicals were purchased from Sigma-Aldrich and used without further purification. 2-Amino-3-[(2-pyridylmethyl)amino]-2(Z)-butene-1,4-dinitrile[20] and 1-(3-formyl-4-hydroxyphenylazo)-4-nitrobenzene[27] were synthesized according to literature methods. Electronic spectral measurements were carried out using Optizen 3220 UV spectrophotometer in the range of 200-900 nm. FT-IR spectra were recorded as pressed KBr discs, using Unicom Galaxy Series FT-IR 5000 spectrophotometer in the region of 400-4000 cm^{-1}. Melting points were determined on Electrothermal 9200 apparatus. NMR spectra were recorded on Bruker AV 300 MHz and Bruker Avance III 400 MHz spectrometers. C. H. N. analyses were performed on a Vario EL III elemental analyzer.

Synthesis of 2-((*E*)-2-hydroxy-5-((*E*)-(4-nitrophenyl)diazenyl)benzylideneamino)-3-(pyridin-2-ylmethylamino)maleonitrile (1)

A mixture of 1-(3-formyl-4-hydroxyphenylazo)-4-nitrobenzene (0.40 g, 1.5 mmol) and 2-Amino-3-[(2-pyridylmethyl)amino]-2(Z)-butene-1,4-dinitrile (0.20 g, 1 mmol) in MeOH (100 mL) was heated to reflux for 5 h in presence of CF_3COOH (3 drops). The mixture was filtered whilst hot and the obtained solid was washed with hot ethanol (three times) and then with diethyl ether. The resulted product was dried in air. Yield: 89%, m. p. 218-220 ºC. ^1H NMR (DMSO-d_6, 400 MHz, ppm): δ 4.73 (d, 2H, J =6.40 Hz), 7.16 (d, 1H, J = 8.80 Hz), 7.35 (dd, 1H, J = 6.80 Hz and 4.80 Hz), 7.43 (d, 1H, J = 8.00 Hz), 7.84 (td, 1H, J = 7.60 Hz and 1.60 Hz), 7.94 (dd, 1H, J = 8.80 Hz and 2.40 Hz), 8.00 (d, 2H, J = 8.80 Hz), 8.44 (d, 2H, J = 8.80 Hz), 8.60 (d, 1H, J = 4.80 Hz), 8.69 (s, 1H), 8.80 (s, 1H), 8.84 (t, 1H, J = 6.40 Hz, NH), 11.58 (br, 1H, OH). IR (KBr, cm^{-1}); 3271 (NH), 2210 and 2239 (CN), 1618 (C=N), 1601 (C=C), 1556 (C=N pyridine), 1521 (NO_2), 1485 (N=N), 1338 (NO_2), 1282, 1143, 1103, 856, 746 and 686. Anal. Calcd. for $C_{23}H_{16}N_8O_3$: C, 61.06; N, 24.77; H, 3.56. Found: C, 60.41; N, 24.36; H, 3.44 %. λ_{max} (nm) (ε ($M^{-1}cm^{-1}$)): 269 (11200), 397 (35200) and 610 (17250) in DMSO.

Acknowledgements

We are grateful to the Arak University for financial support of this work.

Notes and references

1 A. Aviram, *J. Am. Chem. Soc*., 1988, **110** , 5687-5692.

2 A. P. de Silva, H. Q. N. Gunaratne and C. P. McCoy, *Nature,* 1993, **364** , 42-44.

3 (*a*) Z. Dong, X. Tian, Y. Chen, J. Hou and J. Ma, *RSC Adv*., 2013, **3**, 2227-2233; (*b*) U. Pischel, J. Andre´asson, D. Gust and V. F. Pais, *ChemPhysChem*, 2013, **14**, 28–46; (*c*) R. Gotor, A. M. Costero, S. Gil, M. Parra, P. Gaviña and K. Rurack, *Chem. Commun*., 2013, **49**, 11056-11058.

4 (*a*) N. Kaur and S. Kumar, *Dalton Trans.*, 2012, **41**, 5217-5224; (*b*) D. Margulies, G. Melman and A. Shanzer, *J. Am. Chem. Soc*., 2006, **128**, 4865-4871; (*c*) L. Fu, L. Cao, Y. Liu and D. Zhu, *Adv. Colloid Interface Sci.,* 2004, **111**, 133-157; (*d*) P. Mahato, S. Saha and A. Das, *J. Phys. Chem. C,* 2012, **116**, 17448-17457; (*e*) A. K. Mandal, P. Das, P. Mahato, S. Acharya and A. Das, *J. Org. Chem.,* 2012, **77**, 6789-6800; (*f*) R. Kumar, V. Bhalla and M. Kumar, *Dalton Trans.*, 2013, **42**, 8808-8814.

5 (*a*) H. Wang, H. Wu, L. Xue, Y. Shi and X. Li, *Org. Biomol. Chem.*, 2011, **9**, 5436-5444; (*b*) M. A. Kaloo and J. Sankar, *New J. Chem.*, 2014, **38**, 923-926; (*c*) S. Goswami, A. Manna, S. Paul, K. Aich, A. K. Das and S. Chakraborty, *Dalton Trans.*, 2013, **42**, 8078-8085; (*d*) X. Zhao and C. Z. Huang, *Analyst*, 2010, **135**, 2853-2857; (*e*) R. Guliyev, S. Ozturk, Z. Kostereli and E. U. Akkaya, *Angew. Chem., Int. Ed.,* 2011, **50**, 9826-9831; (*f*) B. Kumar, M. A. Kaloo, A. R. Sekhar and J. Sankar, *Dalton Trans.,* 2014, **43**, 16164-16168; (*g*) R. Martins, P. Barquinha, L. Pereira, N. Correia, G. Gonçalves, I. Ferreira and E. Fortunato, *Appl. Phys. Lett.,* 2008, **93**, 203501–203503; (*h*) F. Galindo, J. C. Lima, S. V. Luis, A. J. Parola and F. Pina, *Adv. Funct. Mater.,* 2005, **15**, 541–545; (*i*) W. Lu, M. Zhang, K. Liu, B. Fan, Z. Xia and L. Jiang, *Sens. Actuators, B,* 2011, **160**, 1005–1010.

6 (*a*) D. Gust, J. Andre´asson, U. Pischel, T. A. Moore and A. L. Moore, *Chem. Commun.,* 2012, **48**, 1947–1957; (*b*) D. Karak, S. Das, S. Lohar, A. Banerjee, A. Sahana, I. Hauli, S. K. Mukhopadhyay, D. A. Safin, M. G. Babashkina, M. Bolte, Y. Garcia and D. Das, *Dalton Trans.*, 2013, **42**, 6708−6715; (*c*) S. Uchiyama, N. Kawai, A. P. de Silva and K. Iwai, *J. Am. Chem. Soc.,* 2004, **126**, 3032-3033; (*d*) G. Nishimura, K. Ishizumi, Y. Shiraishi and T. Hirai, *J. Phys. Chem. B*, 2006, **110**, 21596-21602; (*e*) S. Uchiyama, G. D. McClean, K. Iwaiand A. P. de Silva, *J. Am. Chem. Soc.,* 2005, **127**, 8920-8921; (*f*) M. Kluciar, R. Ferreira, B. de Castro and U. Pischel, *J. Org. Chem.,* 2008, **73**, 6079-6085; (*g*) C. H. Xu, W. Sun, Y. R. Zheng, C. J. Fang, C. Zhou, J. Y. Jin and C. H. Yan, *New J. Chem.,* 2009, **33**, 838−846.

7 (*a*) A. P. de Silva and N. D. McClenaghan, *Chem.–Eur. J.,* 2002, **8**, 4935–4945; (*b*) Q. A. Bozdemir, R. Guliyev, N. Buyukcakir, S. Selcuk, S. Kolemen, G. Gulseren, T. Nalbantoglu, H. Boyaci and E. U. Akkaya, *J. Am. Chem. Soc.*, 2010, **132**, 8029–8036; (*c*) D. C. Magri, G. J. Brown, G. D. McClean and A. P. de Silva, *J. Am. Chem. Soc.,* 2006, **128**, 4950–4951.

8 Y.-L. Zhu, T. Huang, Q. Zhang, Y. Huang and J.-B. Wu, *Chin. J. Inorg. Chem.*, 2011, **27**, 1471–1476.

9 (*a*) Madhuprasad, N. Swathi, J. R. Manjunatha, U. K. Das, A. N. Shetty and D. R. Trivedi, *New J. Chem.,* 2014, **38**, 1484–1492; (*b*) C. Mannel-Croise, C. Meister and F. Zelder, *Inorg. Chem.,* 2010 , **49**, 10220-10222; (*c*) R. Kumar, V. Bhalla and M. Kumar, *Tetrahedron*, 2008 , **64**, 8095-8101; (*d*) V. Bhalla, R. Tejpal and M. Kumar, *Tetrahedron*, 2011 , **67**, 1266-1271; (*e*) P. G. Sutariya, A. Pandya, A. Lodha and S. K. Menon, *Analyst* , 2013, **138** , 2531-2535.

10 (*a*) V. Luxami and S. Kumar, *RSC Adv.,* 2012 , **2**, 8734-8740; (*b*) K. K. Upadhyay, A. Kumar, R. K. Mishra, T. M. Fyles, S. Upadhyay and K. Thapliyal, *New J. Chem.,* 2010 , **34** , 1862-1866; (*c*) Y. Liu, M. Li, Q. Zhao, H. Wu, K. Huang and F. Li, *Inorg. Chem.,* 2011 , **50**, 5969-5977.

11 (*a*) L. Wang, B. Li, L. Zhang and Y. Luo, *Dalton Trans.*, 2013, **42**, 459-465; (*b*) Y. Shiraishi, Y. Tokitoh and T. Hirai, *Chem. Commun.*, 2005, **42** , 5316-5318; (*c*) V. Luxami and S. Kumar, *Dalton Trans.*, 2012, **41**, 4588-4593.

12 K. C. Chang, I. H. Su, Y. Y. Wang and W. S. Chung, *Eur. J. Org. Chem.,* 2010, 4700-4704.

13 J. Wang and C.-S. Ha, *Sens. Actuators, B*, 2010, **146**, 373-380.

14 (*a*) I. Guezguez, A. Ayadi, K. Ordon, K. Iliopoulos, D. G. Branzea, A. Migalska-Zalas, M. Makowska-Janusik, A. El-Ghayoury and B. Sahraoui, *J. Phys. Chem. C*, 2014, **118**, 7545−7553; (*b*) H. Khanmohammadi and K. Rezaeian, *RSC Adv.,* 2014, **4**, 1032-1038;

(*c*) S. Uruş, S. Purtaş, G. Ceyhan and F. Tümer, *Chem. Eng. J.,* 2013, **220**, 420-430; (*d*) E. İspir, *Dyes Pigments,* 2009, **82**, 13-19; (*e*) A. K. Singh, J. Das and N. Majumdar, *J. Am. Chem. Soc.,* 1996, **118**, 6185-6191; (*f*) A. K. Mahapatra, S. K. Manna, K. Maiti, R. Maji, C. D. Mukhopadhyay, D. Sarkar and T. K. Mondal, *RSC Adv.,* 2014, **4**, 36615-36622.

15 H. A. Benesi and J. H. Hildebrand, *J. Am. Chem. Soc*., 1949, **71**, 2703–2707.

16 (*a*) T. P. Lin, C. Y. Chen, Y. S. Wen and S. S. Sun, *Inorg. Chem.,* 2007, **46**, 9201–9212; (*b*) R. Sakai, E. B. Barasa, N. Sakai, S. Sato, T. Satoh and T. Kakuchi, *Macromolecules*, 2012, **45**, 8221-8227; (*c*) L. Wang, X. He, Y. Guo, J. Xu and S. Shao, *Org. Biomol. Chem.,* 2011, **9**, 752–757.

17 W. T. Gong, Q. L. Zhang, L. Shang, B. Gao and G. L. Ning, *Sens. Actuators, B,* 2013, **177**, 322-326.

18 C. Jin, M. Zhang, C. Deng, Y. Guan, J. Gong, D. Zhu, Y. Pan, J. Jiang and L. Wang, *Tetrahedron Lett.,* 2013, **54**, 796-801.

19 (*a*) V. K. Gupta, A. K. Singh, M. R. Ganjali, P. Norouzi, F. Faridbod and N. Mergu, *Sens. Actuators, B,* 2013, **182**, 642-651; (*b*) R. Sheng, P. Wang, Y. Gao, Y. Wu, W. Liu, J. Ma, H. Li and S. Wu, *Org. Lett.,* 2008, **10**, 5015–5018.

20 L. S. Beall, N. S. Mani, A. J. P. White, D. J. Williams, A. G. M. Barrett and B. M. Hoffman, *J. Org. Chem.,* 1998, **63**, 5806-5817.

21 (*a*) M. Bala and A. I. P. Sinha, *Asian J. Chem.,* 1989, **1**, 392-400; (*b*) H. Keypour, H. Khanmohammadi, K. P. Wainwright and M. R. Taylor, *Inorg. Chim. Acta*, 2003, **355**, 286-291.

22 (*a*) A. Helal, S. H. Kim and H. S. Kim, *Tetrahedron*, 2010, **66**, 9925-9932; (*b*) M. Shellaiah, Y. H. Wu and H. C. Lin, *Analyst*, 2013, **138**, 2931–2942; (*c*) R. K. Pathak, V. K. Hinge, A. Rai, D. Panda and C. P. Rao, *Inorg. Chem.*, 2012, **51**, 4994-5005.

23 (*a*) D. Maity, A. K. Manna, D. Karthigeyan, T. K. Kundu, S. K. Pati and T. Govindaraju, *Chem. Eur. J.*, 2011, **17** , 11152-11161; (*b*) Z. Li, L. Zhang, L. Wang, Y. Guo, L. Cai, M. Yu and L. Wei*, Chem. Commun.*, 2011, **47** , 5798-5800.

24 (*a*) A. F. Li, Y. B. Ruan, Q. Q. Jiang, W. B. He and Y. B. Jiang, *Chem. Eur. J.,* 2010, **16**, 5794-5802; (*b*) M. de Sousa, B. de Castro, S. Abad, M. A. Miranda and U. Pischel, *Chem. Commun.*, 2006, 2051-2053; (*c*) P. Singh and S. Kumar, *New J. Chem.,* 2006, **30**, 1553-1556.

25 (*a*) P. Kaur, S. Kaur and K. Singh, *Org. Biomol. Chem.,* 2012, **10**, 1497-1501; (*b*) X. Tian, Z. Dong, J. Hou, R. Wang and J. Ma, *J. Lumin.,* 2014, **145**, 459–465.

26 (*a*) N. Sharma, S. I. Reja, V. Bhalla and M. Kumar, *Dalton Trans.,* 2014, **43**, 15929–15936; (*b*) S. Pramanik, V. Bhalla and M. Kumar, *ACS Appl. Mater. Interfaces*, 2014, **6**, 5930–5939.

27 H. Khanmohammadi and M. Darvishpour, *Dyes Pigments,* 2009, **81**, 167-173.